Supplementary Information

Microfluidic harvesting of breast cancer tumor spheroid-derived extracellular vesicles from immobilized microgels for single-vesicle analysis

Xilal Y. Rima,[1] Jingjing Zhang,[1] Luong T. H. Nguyen,[1] Aaron Rajasuriyar,[1] Min Jin Yoon,[1] Chi-Ling Chiang,[1] Nicole Walters,[1] Kwang Joo Kwak,[2] L. James Lee,[1,2] and Eduardo Reátegui[1,3*]

[1] William G. Lowrie Department of Chemical and Biomolecular Engineering, The Ohio State University, Columbus OH 43210

[2] Spot Biosystems LLC, Palo Alto, CA, USA

[3] Comprehensive Cancer Center, The Ohio State University, Columbus, OH 43210

[*]Corresponding Author: reategui.8@osu.edu

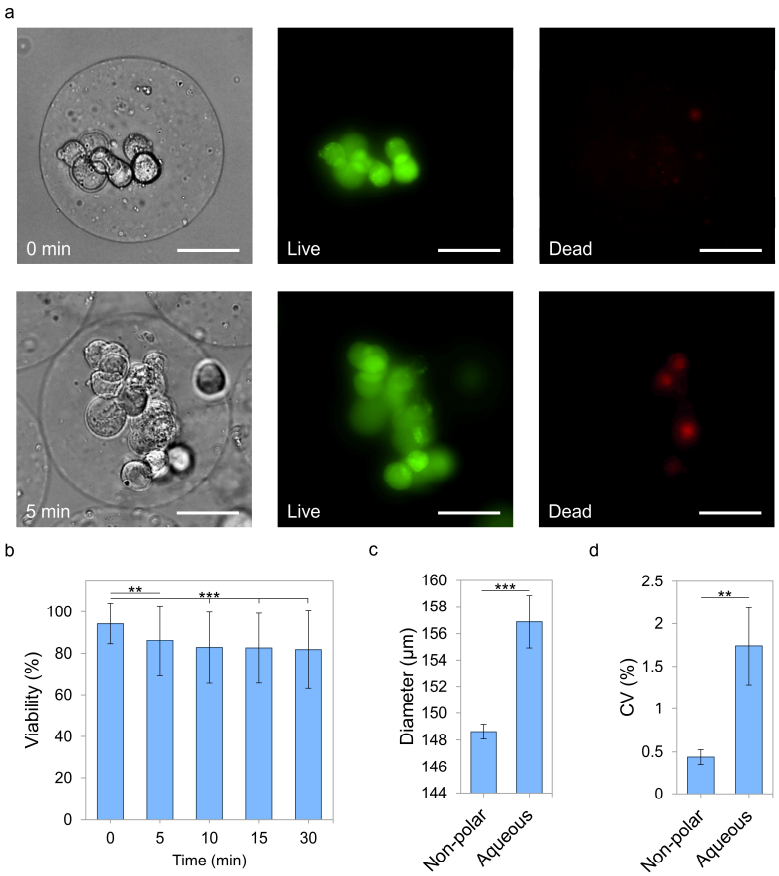

Supplementary Figure 1: Microdroplet alterations post-gelation. (a) Brightfield images demonstrate MCF7 cells encapsulated within gelled EV microbioreactors (^{EV}µBRs) for both an instant incubation and a 5 min incubation in 0.04 % acetic acid for internal gelation (left). Live cells were stained green with calcein-AM (center). Dead cells were stained red with ethidium homodimer-1 (right). **(b)** Cellular viability decreases with increasing incubation times of 0.04 % acetic acid for internal microdroplet gelation. Viabilities are 94.31 ± 9.85 %, 86.05 ± 16.75 %, 82.73 ± 16.99 %, 82.52 ± 16.70 %, and 81.79 ± 18.51 % for 0 min, 5 min, 10 min, 15 min, and 30 min, respectively (n = 100, error bars indicate the standard deviation). **(c)** The diameter of the microdroplets increases from 148.62 ± 0.55 µm to 156.86 ± 1.98 µm post-gelation (n = 100, error bars indicate the standard deviation). **(d)** The coefficient of variation (CV) of the microdroplets

increases from 0.44 ± 0.08 % to 1.73 ± 0.46 % post-gelation (n = 3, error bars indicate the standard deviation). All scale bars are 50 µm (**p-value < 0.005, ***p-value < 0.0001).

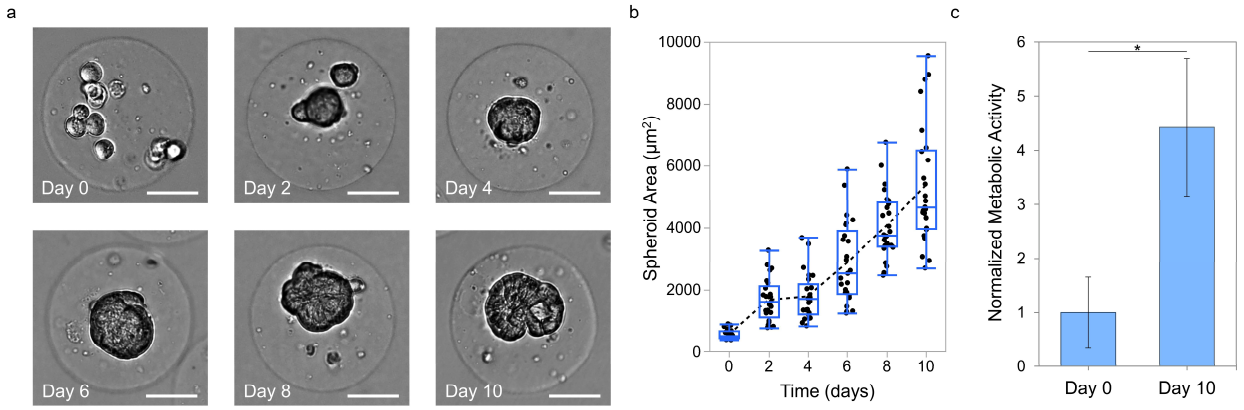

Supplementary Figure 2: Formation of tumor spheroids within ^{EV}µBRs. (a) Single suspended MCF7 cells within the ^{EV}µBRs aggregate and develop tumor spheroids, which continually grow over 10 days. **(b)** The corresponding boxplots (n = 25) of tumor spheroid growth over 10 days demonstrates a steady increase in area, proceeding single-cell aggregation. **(c)** The metabolic activity (relative to day 0) increases from 1.00 ± 0.66 to 4.42 ± 1.27 (n = 3, error bars indicate the standard deviation). All scale bars are 50 µm (*p-value < 0.05).

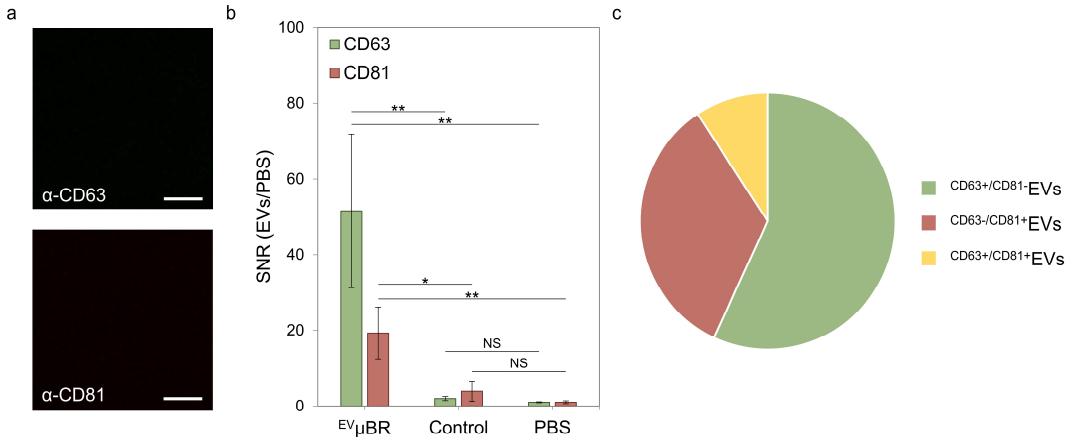

Supplementary Figure 3: Detection of differentially expressed tetraspanins on single-EVs harvested from the microfluidic system. (a) TFF-purified media, serving as the negative control, demonstrates an absence of fluorescent signal for α-CD63 and α-CD81 detection antibodies. **(b)** The SNR ratio depicts a significant increase in signal from ^{EV}μBRs and a slight insignificant increase in the negative control. **(c)** The pie chart illustrates the distribution of EVs derived from the microfluidic system. All scale bars are 5 μm (**p*-value < 0.05, ***p*-value < 0.005).

Supplementary Video 1: Flow-focusing phase mixing. The sodium-alginate stream containing MCF7 cells is introduced through the top of the top junction and the sodium-alginate stream containing 50 nm $CaCO_3$ nanoparticles is introduced through the sides of the top junction, where the streams combine via laminar flow. The dispersed phase then meets the continuous phase containing a fluorosurfactant diluted in a hydrofluoroether at the bottom junction to form microdroplets. The scale bar is 100 µm.

Supplementary Video 2: Hydrodynamic locking mechanism of ^{EV}µBRs. The tumor spheroid encapsulated within an ^{EV}µBR is halted at the entrance of the hydrodynamic trap, then deformed by increasing the flow rate, and locked into place within the hydrodynamic trap. The scale bar is 100 µm.